

—Original Article—

## Pterostilbene alleviates hydrogen peroxide-induced oxidative stress via nuclear factor erythroid 2 like 2 pathway in mouse preimplantation embryos

Obaid ULLAH<sup>1)\*</sup>, Zhongshu LI<sup>1)\*</sup>, Ihsan ALI<sup>1)\*</sup>, Lijie XU<sup>1)</sup>, Haixing LIU<sup>1)</sup>, Syed Zahid Ali SHAH<sup>2)</sup> and Nanzhu FANG<sup>1)</sup>

<sup>1)</sup>Department of Animal Science, Agricultural College, Yanbian University, Jilin Province 133002, China

<sup>2)</sup>National Animal Transmissible Spongiform Encephalopathy Laboratory, Key Laboratory of Animal Epidemiology and Zoonosis of Ministry of Agriculture, College of Veterinary Medicine and State Key Laboratory of Agrobiotechnology, China Agricultural University, Beijing 100193, China

**Abstract.** Pterostilbene (PTS) in blueberries is a phytoalexin with antioxidant properties. PTS exerts strong cytoprotective effects on various cells via Nuclear Factor Erythroid 2 like 2 (NFE2L2) pathway. We evaluated the antioxidant PTS treatment in mouse preimplantation embryos. *In vitro* culture media were supplemented with different concentrations of PTS. Treatment of zygotes with 0.25  $\mu\text{M}$  PTS improved the development of day 4 blastocysts ( $P < 0.05$ ). Moreover,  $\text{H}_2\text{O}_2$  treatment significantly increased the reactive oxygen species level and reduced the glutathione level in mouse blastocyst, whereas PTS treatment counteracted these effects. The fluorescence intensity of apoptotic positive cell was higher in the  $\text{H}_2\text{O}_2$  group than in the PTS group. Furthermore, PTS-treated embryos significantly increased the protein expression of NFE2L2 in the nucleus and decreased Kelch-like ECH-associated protein1 (KEAP1). PTS treatment significantly increased the expression of downstream target genes involved in the NFE2L2 pathway, such as catalase (CAT), heme oxygenase1 (HMOX1), glutathione peroxidase (GPX), and superoxide dismutase (SOD); these genes confer cellular protection. In addition, PTS treatment significantly increased the expression of anti-apoptotic B-cell lymphoma 2 (BCL2), with a concomitant reduction in the apoptotic Bcl-2-associated X protein (BAX) and *Caspase-3 genes* in the embryo. PTS treatment also increased the protein expression of BCL2 and reduced the protein expression of BAX in the mouse embryo. In conclusion, PTS activated NFE2L2 signaling pathway in the development of mouse embryos by altering downstream expression of genes involved in the antioxidant mechanisms and apoptosis.

**Key words:** *In vitro* culture medium, Mouse embryo, Nuclear Factor Erythroid 2 like 2 (NFE2L2), Oxidative stress, Pterostilbene

(J. Reprod. Dev. 65: 73–81, 2019)

**P**hytochemicals of the polyphenolic structure are generally called natural polyphenols. These phytochemicals are accessory metabolites of plants, thus taking an active part in the protection of plants against various sorts of stresses including high/low temperatures, ultraviolet light radiation, severe drought, low soil fertility, pathogens, and grazing pressure [1]. Polyphenols are abundant micronutrients in our diet, and evidence for their role in disease prevention, such as cancer and cardiovascular disorders, is increasing. Their potential health benefits for humans, including antioxidant properties, are abundant [2].

Natural stilbenes and flavonoids manifest significant antioxidant activity, as proven in numerous cell and mouse models. Quercetin

restrained copper-mediated and azo-initiated low-density lipoprotein oxidation [3]. Resveratrol has a protective effect on mouse embryos against nicotine-induced teratogenesis [4]. Piceatannol reduced hydroxyl radicals in L1210, K562, and HL-60 leukemic cells [5]. A natural analog of resveratrol, pterostilbene (PTS), found primarily in rabbiteye blueberries, deerberry, *Pterocarpus marsupium* heartwood, and grapes [6], is effective in peroxy radical scavenging activities [7]. PTS also possesses a protective effect on normal human fibroblast membrane against lipid peroxidation [8]. PTS exhibits different types of pharmacologic activities, including anti-inflammatory, anti-diabetic, anticancer, and antioxidant activities [9]. Resveratrol and PTS have a similar structure [10], whereas PTS has good metabolic stability and oral absorption due to its only one hydroxyl group [11]. The PTS lipophilicity is enhanced due to the dimethyl ether structure, thereby leading to its increased membrane permeability; thus, it possesses improved pharmacokinetic profiles over resveratrol [6]. PTS scavenged the intracellular free radical and decreased the oxidative stress in diabetic rats [12]. PTS also scavenged the intracellular reactive oxygen species (ROS) generation within the osteoclast precursors during receptor activator of nuclear factor kappa-B ligand-stimulated osteoclastogenesis [13].

Received: July 26, 2018

Accepted: November 2, 2018

Published online in J-STAGE: November 15, 2018

©2019 by the Society for Reproduction and Development

Correspondence: N Fang (e-mail: nzfang@ybu.edu.cn)

\* O Ullah, Z Li and I Ali contributed equally to this study.

This is an open-access article distributed under the terms of the Creative Commons Attribution Non-Commercial No Derivatives (by-nc-nd) License. (CC-BY-NC-ND 4.0: <https://creativecommons.org/licenses/by-nc-nd/4.0/>)

The capabilities of reproductive technologies, such as *in vitro* fertilization, somatic cell nuclear transfer, and intracytoplasmic sperm injection rely on consistent good quality embryo production [14]. Thus, obtaining a valuable embryo culture is important. Despite the significant improvement in embryo culture conditions, the quality of *in vitro*-produced embryos is still sub-optimal [15]. This is due to the fact that the preimplantation embryo is extremely sensitive to high oxygen atmosphere and external environment. Deficiencies in culture condition often lead to ROS generation, which manifests low frequency of blastocyst formation and low cell numbers [16]. Therefore, a culture system that can potentially improve the development of preimplantation embryos is needed.

A handful number of antioxidants, such as  $\beta$ -mercaptoethanol ( $\beta$ -ME), cysteine [17], cysteamine [18], melatonin [19, 20], and resveratrol [21, 22], are used to the *in vitro*-matured oocytes and *in vitro* culture media to improve the developmental competence of preimplantation embryos. In the current study, we used PTS due to its greater potency than resveratrol in terms of anti-oxidative and absorption rates [23]. Recently, Kosuru *et al.* [24] revealed that PTS protects cells from oxidative damage via Nuclear Factor Erythroid 2 like 2 (NFE2L2) pathway. NFE2L2 remains an important master regulator of cytoprotective and antioxidant genes. During normal cellular condition, Kelch-like ECH-associated protein-1 (KEAP1) represses NFE2L2-dependent transcriptional activity. When cells are exposed to oxidative stress, the KEAP1–NFE2L2 pathway is activated, leading to the nuclear translocation of the NFE2L2 from the cytoplasm [25]. Thus, it activates downstream anti-oxidant genes to maintain cellular redox homeostasis [26]. In this study, we investigated the protective role of PTS during *in vitro* culture in mouse preimplantation embryos, ROS, glutathione (GSH) levels, tunel assay, the KEAP1–NFE2L2 pathway activation, and the apoptotic expression of BCL2 family in mouse blastocyst.

## Materials and Methods

### Chemicals and reagents

Unless otherwise stated, all chemicals and reagents used in the present study were obtained from Sigma-Aldrich (St. Louis, MO, USA). PTS was purchased from Cayman Chemical Michigan, USA (Cat no. 537-42-8).

### Animal ethics statement

This study was carried out in strict accordance with Yanbian University's guidelines for the care and use of animals. All experimental procedures were approved by the committee on the ethics of animal experiments at Yanbian University.

### Superovulation, embryo collection, and *in vitro* culture

Kunming mice (*Mus musculus*), which originated from Swiss albino mouse [27], were acquired from the experimental animal center of Yanbian University. Healthy mice of 8–10 weeks old were housed under conditions of 12 h light and 12 h dark cycle (12:12). Nulliparous females were superovulated via intraperitoneal injection of 10 IU pregnant mare serum gonadotropin (Ningbo Hormone, Ningbo, China; Cat no. 140825), followed by 10 IU human chorionic gonadotropin (hCG; Ningbo Hormone; Cat no. 140913) after 48 h

later and mated with a single fertile male of the same strain. After 12 h, the vaginal plug was checked and defined as day zero of gestation. Mice with plugs were sacrificed after 22 h of hCG injection. The zygotes were obtained by extraction of oviducts and placed in an M<sub>2</sub> medium (Cat no. M7167, Sigma-Aldrich) under a stereo microscope. Cumulus cells were removed with 0.03% hyaluronidase (H3506, Sigma-Aldrich) and washed with M<sub>2</sub> medium. To determine the protective effect of PTS against oxidative stress, zygotes (n = 5 each) in the 25  $\mu$ l drops of M<sub>16</sub> medium (Cat no. M7292, Sigma-Aldrich) were supplemented with various concentrations of PTS (0, 0.1, 0.25, 0.5, 0.75, and 1  $\mu$ M) covered with mineral oil under 37°C under 5% CO<sub>2</sub> in 95% humidified air. The experiment was replicated six times in each group. A concentration of 0.25  $\mu$ M PTS significantly promoted the percentage of blastocyst development (P < 0.05, Table 2). Therefore, PTS at the concentration of 0.25  $\mu$ M was used for further analysis. The zygotes were collected and divided into three groups. The first group zygotes were cultured in 25  $\mu$ l drops of the M<sub>16</sub> medium group. The zygotes in the second and third groups were cultured in 25  $\mu$ l of M<sub>16</sub> medium containing 10  $\mu$ M hydrogen peroxide (H<sub>2</sub>O<sub>2</sub>) and 10  $\mu$ M H<sub>2</sub>O<sub>2</sub> plus 0.25  $\mu$ M PTS covered with mineral oil, respectively. All embryos were incubated at 37°C under water-saturated 5% CO<sub>2</sub> in the air. Embryonic development was observed every 24 h.

### Measurement of GSH and ROS levels

To detect the intracellular GSH and ROS levels, 20 embryos at day 4 blastocysts from each treated group were washed twice with polyvinyl alcohol (1 mg/ml) and then incubated for 15 min in 50  $\mu$ l of a droplet of 10  $\mu$ M 4-chloromethyl-6, 8-difluoro-7-hydroxycoumarin (CMF2HC, Cat. No. C12881, Life Technologies, Carlsbad, CA, USA) and 10  $\mu$ M 2,7-dichlorodihydro-fluorescein diacetate (DCHFDA, Cat. No. D6883, Sigma-Aldrich) respectively. After incubation, the embryos were washed twice with phosphate-buffered saline (PBS) and examined under an epifluorescent microscope (IX71 Olympus Tokyo, Japan). GSH had an excitation wavelength of 371 nm emission wavelength of 464 nm. The excitation wavelength and the emission wavelength for ROS were 480 and 510 nm, respectively. The results are shown as the relative intensity of fluorescence. All images were captured under the same conditions. The images were analyzed by image-pro plus 6.0 (Media Cybernetics, Rockville, MD, USA).

### Terminal deoxynucleotidyl transferase dUTP nick-end labeling (TUNEL)

TUNEL assay was performed according to the manufacturer's protocol by using a frag EL™ DNA fragmentation detection kit (Calbiochem, Roche Diagnostics, USA; Cat. No. QIA39). Briefly, fixed blastocysts (n = 20) from each treated group were washed thrice with 4% paraformaldehyde (PFA) (pH 7.4) containing 0.4 g PFA + 10 ml PBS and fixed in 4% PFA for 1 hour at room temperature in the dark. All blastocysts after 96 h were washed thrice with Tris-buffered saline (TBS) and then incubated in permeabilization buffer (0.5%) Triton X-100 for 1 h. After incubation, the blastocysts were washed thrice with TBS and placed in 50  $\mu$ l 1xTdt for 20 min in the dark at room temperature. The blastocysts were then transferred to 50  $\mu$ l of the Tdt labeling reaction mixture (57  $\mu$ l fluorescein-Frag FL Tdt labeling reaction + 3  $\mu$ l Tdt enzyme) and incubated for 1 h. After

**Table 1.** Information on the primers used for RT-PCR

Genes	Access No.	Forward primer (5'-3')	Reverse primer (5'-3')	T <sub>m</sub> (°C)	Amplicon size, bp
<i>GAPDH</i>	BC023196	CATCACCATCTTCCAGGAGCG	GAGGGGCCATCCACAGTCTTC	59	357
<i>HMOX1</i>	NM010442	CAGGTGATGCTGACAGAGGA	ACAGGAAGCTGAGAGTGAGG	62	184
<i>CAT</i>	NM009804	GGAGGCGGGAACCCAATAG	GTGTGCCATCTCGTCAGTGAA	59	102
<i>GPX</i>	NM008160	GTGCGAAGTGAATGGTGAGA	CTGGGACAGCAGGGTTTCTA	59	253
<i>SOD</i>	NM011434	TTCGAGCAGAAGGCAAGCGGTGAA	AATCCCAATCACACCACAAGCCAA	59	396
<i>BAX</i>	NM007527	CCAGGATGCGTCCACCAA	AAGTAGAAGAGGGCAACCAC	62	195
<i>BCL2</i>	NM007527	AACTCTCAGGGATGGGG	GCCGGTTCAGGTACTCAG	59	144
<i>CASP-3</i>	NM001284409	GGAGAAATTCAAAGGACGG	AACAAAACAGAAACACGCC	59	260

**Table 2.** *In vitro* development of mouse embryos with different concentrations of PTS

Treated groups	No. of zygotes cultured †	Percentages of embryos developed to [mean (SEM), %]		
		2-cell	4-cell	Blastocyst
Control	154	97.8 ± 1.4 <sup>a</sup>	80.0 ± 1.35 <sup>a</sup>	44.1 ± 1.68 <sup>a</sup>
PTS (0.10 μM)	151	96.8 ± 2.3 <sup>a</sup>	80.2 ± 1.16 <sup>ac</sup>	44.6 ± 0.79 <sup>a</sup>
PTS (0.25 μM)	151	98.4 ± 0.9 <sup>a</sup>	88.1 ± 1.10 <sup>b</sup>	55.1 ± 0.96 <sup>b</sup>
PTS (0.50 μM)	152	96.8 ± 0.8 <sup>a</sup>	77.6 ± 2.13 <sup>a</sup>	41.6 ± 0.97 <sup>a</sup>
PTS (0.75 μM)	157	93.2 ± 4.8 <sup>a</sup>	74.6 ± 1.74 <sup>ac</sup>	37.1 ± 0.80 <sup>a</sup>
PTS (1.00 μM)	153	93.7 ± 1.9 <sup>a</sup>	68.5 ± 1.64 <sup>c</sup>	33.0 ± 1.09 <sup>c</sup>

<sup>a-c</sup> Values within a column with different superscripts significantly differ ( $P < 0.05$ ). † Experiment was replicated more than 6 times.

being washed thrice with TBS, the blastocysts were mounted into fluorescent media onto glass slides, and their nuclear configuration was analyzed. The numbers of cells per blastocyst were observed immediately using a Nikon microscope (ECLIPSE Ti-s 634268, Nikon, Melville, NY, USA) at 400 × magnification. Photographs were taken using a 1600 ASA color film. The excitation wavelength was 380 nm, and the emission wavelength was 495 nm. TUNEL-positive cells fluoresced green, indicating these cells were apoptotic. Meanwhile, the total number of cells was determined by the extent of blue. The results were shown as the relative intensity of fluorescence.

#### Western blot analysis

Approximately 200 day 4 mouse blastocysts were selected from each group and lysed in a radioimmunoprecipitation assay (Beyotime, Jiangsu, China). Meanwhile, the nuclear and cytoplasmic proteins of blastocysts were extracted with a nuclear protein extraction kit (Cat no. P0027, Beyotime Biotechnology, China) and heated at 95°C for 5 min to evaluate the NFE2L2 expression that contained a protease inhibitor. The total protein concentration in each group was detected on NANODROP one (Thermo Fischer Scientific). Protein lysate from the blastocysts was added to 12% sodium dodecyl sulfate-polyacrylamide gel (SDS-PAGE) electrophoresis. The detached proteins were transferred to polyvinylidene fluoride membranes (Millipore, USA). The membranes were blocked in skim milk for 1 h. Then, the membrane was incubated with primary antibodies KEAP1 rabbit polyclonal antibody (Proteintech; Cat no. 10503-2-AP), NFE2L2 rabbit polyclonal antibody (Proteintech; Cat no. 16396-1-AP), BCL2 rabbit polyclonal antibody (Proteintech; Cat no. 12789-1-AP),

BAX rabbit polyclonal antibody (Proteintech; Cat no. 50599-2-Ig), and glyceraldehyde-3-phosphate dehydrogenase (GAPDH) rabbit polyclonal antibody (Proteintech; Cat no. 10494-1-AP) at 4 °C overnight. Afterward, the membrane in TBST was washed thrice and incubated at room temperature for 2 h with peroxidase-conjugated affinipu goat anti-rabbit IgG (Proteintech; Cat no. SA 00001-2). The target protein bands were detected using a chemiluminescence plus reagent (ECL plus, Bio Sharp Life Science, Cat no. BL520A).

#### RNA isolation, cDNA synthesis, and polymerase chain reaction (PCR)

For RNA isolation, three biological replicates containing 100 blastocysts from each group were used. Total RNA was isolated from mouse embryos by using Qiagen RNeasy mini kit (Qiagen, Hiden, Germany, Cat no. 74104) according to the manufacturer's instruction. cDNA was synthesized by reverse transcription by using prime script™ RT reagent kit with gDNA Eraser (Takara Biotechnology, Dalian, China, Cat no. RR036A). RNA concentration and purity were detected on NANODROP one (Thermo Fischer Scientific). Primer sequence and annealing temperature are listed in Table 1. PCR was performed in 25 μl reaction volume containing 13 μl 2 × Taq PCR master mix (Tiangen Biotech, Beijing, China, Cat no. KT201), 4 μl cDNA, 1 μl forward and reverse primers (5 mM), and 6 μl H<sub>2</sub>O, followed by initial pre-incubation step at 95°C for 3 min, then 35 cycles of denaturation at 95°C for 30 sec, annealing at 59°C to 62°C for 30 sec, extension at 72°C for 30 sec, and a final extension at 72°C for 5 min. The PCR products were separated by electrophoresis on 2% agarose gels and then visualized under UV illumination. The

**Table 3.** *In vitro* development of mouse embryos with different concentrations of H<sub>2</sub>O<sub>2</sub>

Treated groups	No. of zygotes cultured †	Percentages of embryos developed to [mean (SEM), %]		
		2-cell	4-cell	Blastocyst
Control	125	96.2 ± 0.87 <sup>a</sup>	82.3 ± 1.43 <sup>a</sup>	45.0 ± 1.10 <sup>a</sup>
H <sub>2</sub> O <sub>2</sub> (5 μM)	127	88.2 ± 1.02 <sup>a</sup>	78.2 ± 1.96 <sup>a</sup>	38.2 ± 0.80 <sup>a</sup>
H <sub>2</sub> O <sub>2</sub> (10 μM)	126	89.3 ± 1.30 <sup>a</sup>	62.0 ± 2.00 <sup>b</sup>	23.0 ± 1.73 <sup>b</sup>
H <sub>2</sub> O <sub>2</sub> (20 μM)	125	86.4 ± 1.10 <sup>a</sup>	57.5 ± 1.77 <sup>c</sup>	10.0 ± 0.72 <sup>c</sup>

<sup>a-c</sup> Values within a column with different superscripts significantly differ (P < 0.05). † Experiment was replicated more than 5 times.

**Table 4.** Effect of 0.25 μM PTS on early mouse embryonic development induced by H<sub>2</sub>O<sub>2</sub> (10 μM)

Treated groups	No. of zygotes cultured †	Percentages of embryos developed to [mean (SEM), %]		
		2-cell	4-cell	Blastocyst
Control	125	96.0 ± 0.57 <sup>a</sup>	80.3 ± 1.33 <sup>a</sup>	46.0 ± 1.00 <sup>a</sup>
H <sub>2</sub> O <sub>2</sub> -treated	126	88.3 ± 2.30 <sup>a</sup>	64.0 ± 2.20 <sup>b</sup>	22.0 ± 2.10 <sup>b</sup>
H <sub>2</sub> O <sub>2</sub> and PTS-treated	128	96.3 ± 0.57 <sup>a</sup>	79.6 ± 0.33 <sup>a</sup>	44.0 ± 0.57 <sup>a</sup>

<sup>ab</sup> Values within a column with different superscripts significantly differ (P < 0.05). † Experiment was replicated more than 5 times.

band intensities were analyzed by Lane 1D analysis software (Beijing Sage Creation Science, Beijing, China).

### Statistical analysis

All data comparisons were calculated using multiple comparisons in SPSS 17.0 and one-way ANOVA, followed by post-hoc turkey's multiple comparison tests by using GraphPad Prism 5 software (La Jolla, CA, USA). Statistical significance was considered at P < 0.05, and data were performed on three separate occasions.

## Results

### Effect of different PTS concentrations on embryonic development

In a preliminary experiment, we determined the optimum PTS dose. Various PTS concentrations [0, 0.1, 0.25, 0.50, 0.75, and 1.00 μM added to *in vitro* culture (IVC) medium] were used to evaluate the best treatment for further analysis. No significant difference (P < 0.05) was observed in the percentage of embryos that underwent a 2-cell stage among all treated groups. Moreover, the percentage of 4-cell stage embryos was significantly higher (P < 0.05) in 0.25 μM PTS-treated embryos compared with the control and other groups. Furthermore, the percentage of embryos that developed into day 4 blastocysts was significantly higher (P < 0.05) in the group treated with 0.25 μM PTS than in other groups (Table 2). Therefore, PTS was used at a concentration of 0.25 μM for all the subsequent experiments.

### Effects of PTS on the developmental ability of preimplantation embryos

The zygotes at the developmental stage were subjected to 10 μM H<sub>2</sub>O<sub>2</sub> alone (Table 3) and 10 μM H<sub>2</sub>O<sub>2</sub> plus 0.25 μM PTS to evaluate the antioxidant effect of PTS against H<sub>2</sub>O<sub>2</sub>-induced oxidative stress in preimplantation embryos of the mouse (Table 4). No significant

difference was observed between the groups during the cleavage stage (P < 0.05). However, the 4-cell stage rate of embryos exposed to H<sub>2</sub>O<sub>2</sub> was significantly lower (P < 0.05) than in the control and PTS. By contrast, the blastocyst rate was higher (P < 0.05) in the PTS-treated group than in the H<sub>2</sub>O<sub>2</sub>-treated group.

### Effect of PTS on intracellular GSH and ROS levels

The embryos were collected at the blastocyst stage and stained with CMF2HC and DCHFDA to quantify the intracellular level of GSH and ROS (Fig. 1A). The GSH level in the H<sub>2</sub>O<sub>2</sub>-treated group was significantly lower (P < 0.05) in the blastocyst stage compared with the control and those treated with PTS + H<sub>2</sub>O<sub>2</sub> (Fig. 1B). By contrast, the ROS level in embryos treated with H<sub>2</sub>O<sub>2</sub> was significantly higher (P < 0.05) in the blastocyst stage compared with the control and those treated with PTS + H<sub>2</sub>O<sub>2</sub> (Fig. 1B).

### Effect of PTS on a number of total and apoptotic cells

TUNEL assay was performed to evaluate the number of total and apoptotic cells in the blastocyst. TUNEL positive cells fluoresced green, thereby indicating that the cells were apoptotic. Meanwhile, the total number of cells was determined by the extent of a blue color within the blastocyst. The total number of cells per blastocyst was significantly lower (P < 0.05) in the H<sub>2</sub>O<sub>2</sub>-treated group than that in the control and PTS + H<sub>2</sub>O<sub>2</sub>-treated groups (Figs. 2A and 2B). Meanwhile, the number of apoptotic cells per blastocyst was significantly higher (P < 0.05) in the H<sub>2</sub>O<sub>2</sub>-treated group compared with other treatment groups (Fig. 2B).

### Effect of PTS on nuclear translocation of NFE2L2 in the mouse blastocyst

The KEAP1–NFE2L2 system is a cellular self-defense mechanism activated under oxidative stress [28]. To confirm whether PTS activated the KEAP1–NFE2L2 pathway and induced NFE2L2 translocation,

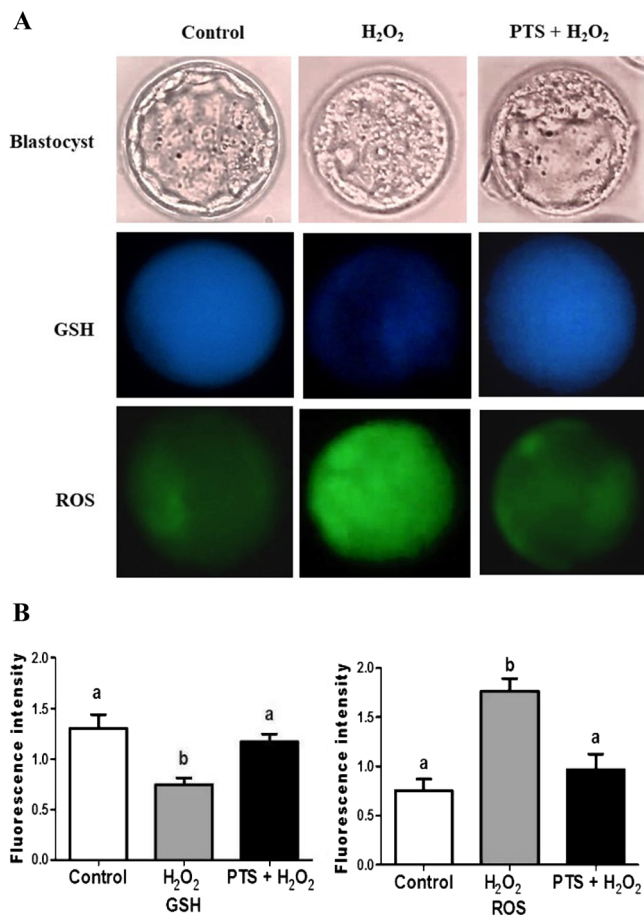


**Fig. 1.** GSH and ROS content in blastocysts. (A) Fluorescence microscopy of the embryo in different cultured media by staining with CMF2HC and DCHFDA. Images are presented at 400 × magnification. (B) fluorescence intensity was quantified by image-pro plus 6.0. Data are expressed as a mean value ± standard error of the mean (SEM) of three independent experiments. <sup>ab</sup> Values with different superscripts in the same column were significantly different ( $P < 0.05$ ).

we added PTS in H<sub>2</sub>O<sub>2</sub>-induced stressed mouse embryos. KEAP1, nuclear, and cytoplasmic extracts of NFE2L2 protein expression in mouse blastocyst were evaluated. KEAP1 protein expression in the PTS + H<sub>2</sub>O<sub>2</sub>-treated group was significantly lower ( $P < 0.05$ ) compared with that in the H<sub>2</sub>O<sub>2</sub>-treated group (Figs. 3A and 3B). By contrast, nuclear NFE2L2 protein expression in PTS was significantly higher ( $P < 0.05$ ) compared with that in the H<sub>2</sub>O<sub>2</sub>-treated group (Figs. 3A and 3C). However, the protein level of NFE2L2 decreased in the cytoplasmic extracts compared with the H<sub>2</sub>O<sub>2</sub>-treated group in day 4 mouse blastocyst (Figs. 3A and 3D). PTS induces NFE2L2 activation and nuclear translocation in the mouse blastocyst.

#### Effect of PTS on NFE2L2 downstream target genes expression

We investigated the gene expression of antioxidant enzymes downstream of NFE2L2 activation and nuclear translocation. The PTS + H<sub>2</sub>O<sub>2</sub>-treated group significantly increased the expression of heme

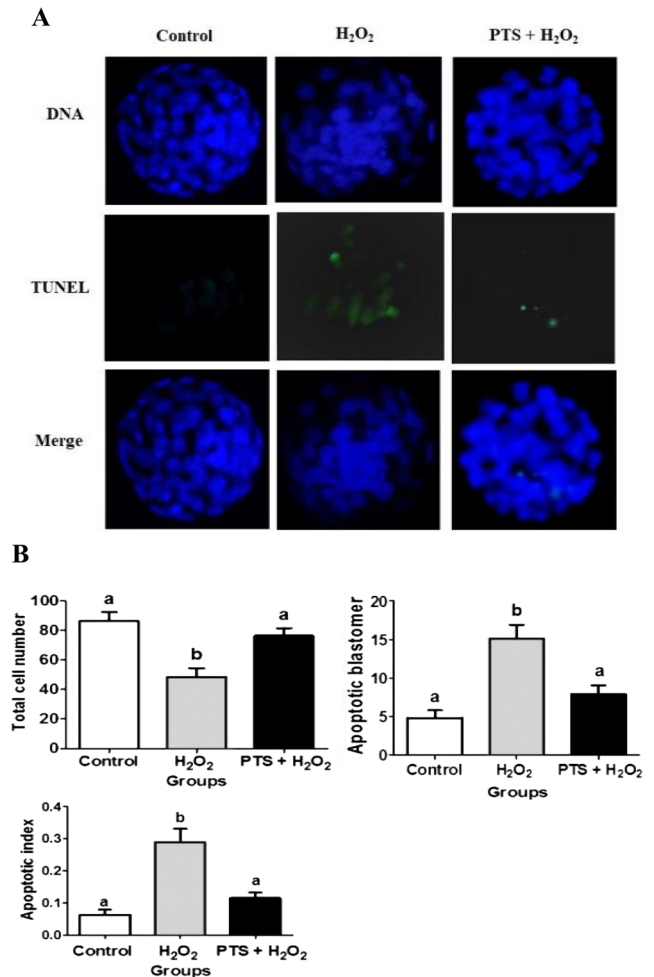


**Fig. 2.** Representative apoptosis images in mouse preimplantation embryos. (A) Apoptotic cells in mouse blastocyst were evaluated by TUNEL assays; counterstained with DAPI. Images are presented at 400 × magnification. (B) The total cell numbers, apoptotic blastomeres, and apoptotic index. (apoptotic index = apoptotic cell/ total cell in a blastocyst). Data are expressed as a mean value ± standard error of the mean (SEM) of three independent experiments. <sup>ab</sup> Values with different superscripts in the same column were significantly different ( $P < 0.05$ ).

oxygenase1 (*HMOX1*), catalase (*CAT*), glutathione peroxidase (*GPX*), and superoxide dismutase (*SOD*) (Figs. 4A and 4B) compared with the H<sub>2</sub>O<sub>2</sub>-treated group. PTS enhanced the expression of antioxidant genes triggered by NFE2L2, thereby protecting the mouse embryo against the H<sub>2</sub>O<sub>2</sub>-treated induced oxidative stress.

#### Effect of PTS on apoptotic-related genes in the mouse blastocyst

The effect of PTS treatment on apoptotic gene expression in day 4 mouse blastocysts is shown in Fig. 5A. PTS significantly upregulated the RNA expression of an anti-apoptotic gene, *BCL2* (Figs. 5A and 5B) with a concomitant reduction in the expression of proapoptotic *BAX* and *Caspase-3* compared with the H<sub>2</sub>O<sub>2</sub>-treated groups (Figs. 5A and 5B).

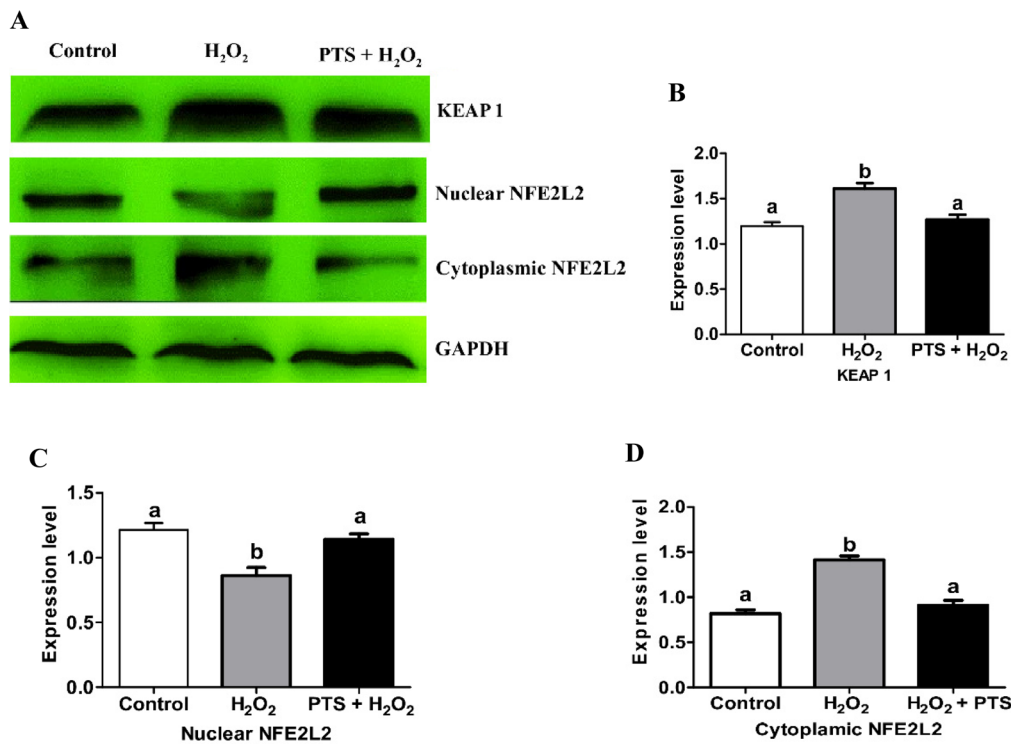


**Fig. 3.** Effect of PTS treatment on NFE2L2 and KEAP1 proteins expressions in mouse embryo cultured in the different treated group. (A) Western blot results of KEAP1, nuclear and cytoplasmic NFE2L2 protein expressions in the mouse blastocyst. (B) Relative expression of KEAP1, nuclear, and cytoplasmic NFE2L2 normalized with the internal marker GAPDH ( $P < 0.05$ ). Data are expressed as a mean value  $\pm$  standard error of the mean (SEM) of three independent experiments. <sup>ab</sup> Values with different superscripts in the same column were significantly different ( $P < 0.05$ ).

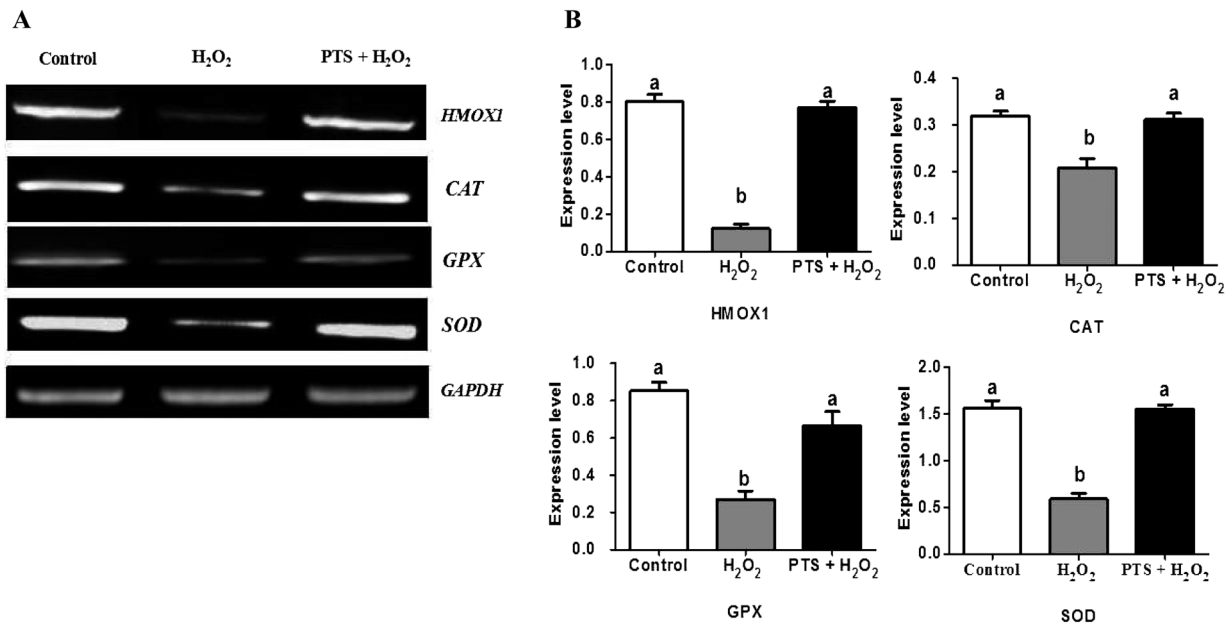


**Fig. 4.** Effect of PTS treatment on expressions of *NFE2L2* downstream genes in mouse embryo cultured in the different treated group. (A) PCR results of *HMOX1*, *CAT*, *GPX*, and *SOD* in the mouse embryo. (B) Relative expressions of *HMOX1*, *CAT*, *GPX*, and *SOD* normalized with the internal marker *GAPDH* ( $P < 0.05$ ). Data are expressed as a mean value  $\pm$  standard error of the mean (SEM) of three independent experiments. <sup>ab</sup> Values with different superscripts in the same column were significantly different ( $P < 0.05$ ).

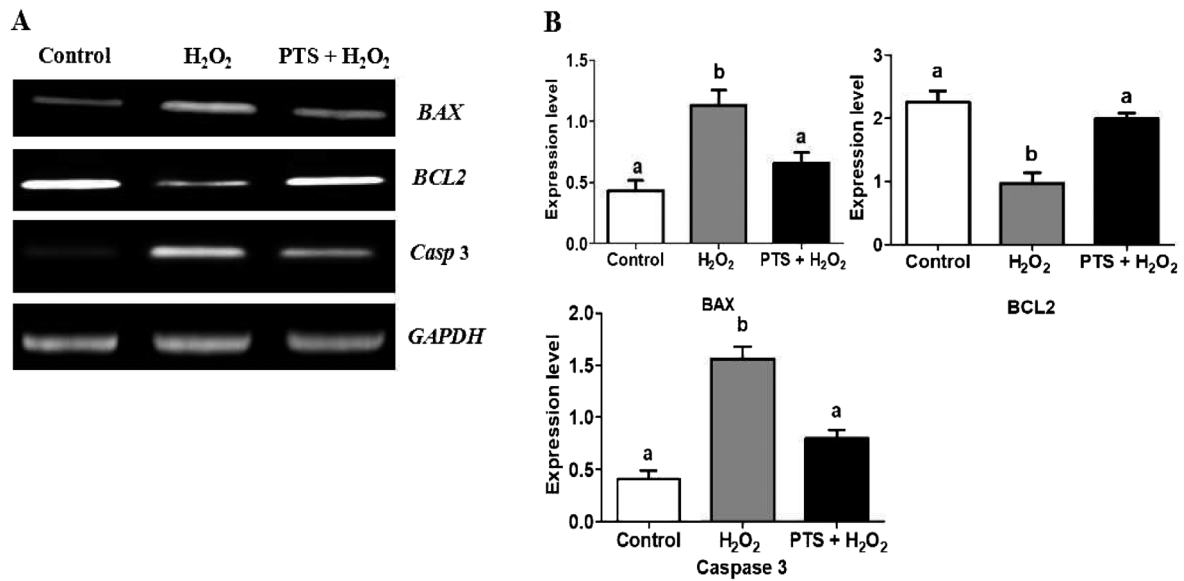


**Fig. 5.** Effect of PTS treatment on *BCL2*, *BAX*, and *Caspase-3* genes expressions in mouse embryo cultured in the different treated group. (A) PCR results of *BCL2*, *BAX*, and *Caspase-3* expressions in control and treated groups in mouse embryos. (B) Relative changes of *BCL2*, *BAX*, and *Caspase-3* normalized with the internal marker *GAPDH* ( $P < 0.05$ ). Data are expressed as a mean value  $\pm$  standard error of the mean (SEM) of three independent experiments. <sup>ab</sup> Values with different superscripts in the same column were significantly different ( $P < 0.05$ ).

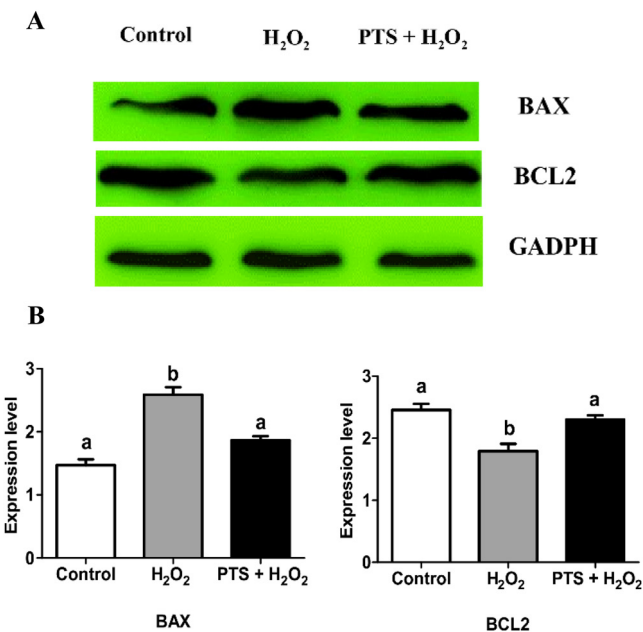


**Fig. 6.** Effect of PTS treatment on *BCL2* and *BAX* proteins expressions in mouse embryo cultured in the different treated group. (A) Western blot results of *BCL2* and *BAX* expressions in control and treated groups in mouse blastocysts. (B) Relative changes of *BCL2* and *BAX* normalized with the internal marker *GAPDH* ( $P < 0.05$ ). Data are expressed as a mean value  $\pm$  standard error of the mean (SEM) of three independent experiments. <sup>ab</sup> Values with different superscripts in the same column were significantly different ( $P < 0.05$ ).

*Effect of PTS on BAX and BCL2 protein expression levels in the mouse blastocyst*

We analyzed the effect of PTS on H<sub>2</sub>O<sub>2</sub>-induced stress on the expression of pro-apoptotic protein BAX and anti-apoptotic protein BCL2. Western blot analysis data found that PTS treatment significantly increased the expression of anti-apoptotic protein BCL2 compared with the H<sub>2</sub>O<sub>2</sub>-treated group (Figs. 6A and 6B) but significantly decreased the expression level of proapoptotic protein BAX compared with the H<sub>2</sub>O<sub>2</sub>-treated group (Figs. 6A and 6B).

**Discussion**

In early embryonic development *in vitro*, oxidative stress-mediated excessive generation of ROS free radicals, leading to increased apoptosis, changes in gene expression, embryonic fragmentation, and reduced embryo quality [29]. Experimental studies showed that ROS generation was elevated in the stage-specific exposure of embryo to *in vitro* culture environment especially in the blastocyst stage because genome profile of blastocyst differs according to the activities of NFE2L2-mediated stress response pathway [30]. For the first time in this study, we investigated the antioxidant potential of PTS, a natural analog of resveratrol, against H<sub>2</sub>O<sub>2</sub>-induced oxidative stress in mouse preimplantation embryo, thereby distinguishing that it possesses a protective effect through the NFE2L2 system. Recent studies also reported that PTS possesses antiperoxidative and antihyperlipidemic activities through the NFE2L2 system in experimental diabetes [31]. Similarly, PTS also recovered streptozotocin-induced diabetes by improving NFE2L2-mediated antioxidant signaling pathway [32]. Indeed, PTS contained powerful, antioxidant, and chemopreventive effects in breast and prostate cancer cell lines [33, 34].

Several studies revealed that the KEAP1–NFE2L2 signaling pathway was most affected when the embryos were exposed to different environments [30, 35]. Different concentrations of PTS (0–1  $\mu\text{M}$ ) were tested in mouse embryonic culture, and the 0.25  $\mu\text{M}$  concentration of PTS increased the blastocyst development compared with other concentrations (Table 2). For further analysis, the 0.25  $\mu\text{M}$  concentration of PTS was added to  $\text{H}_2\text{O}_2$ -induced oxidative stress in mouse preimplantation embryo. Our data demonstrated that PTS, when added to  $\text{H}_2\text{O}_2$ , increased the percentage of embryo development compared with the  $\text{H}_2\text{O}_2$ -treated group (Table 3). PTS reduced the intracellular ROS level in mouse embryos, as observed in a previous study reporting that PTS was an effective scavenger of ROS in chondrocytes [36]. Intracellular GSH plays an important role in maintaining redox homeostasis, detoxifying xenobiotics, and scavenging peroxides [37, 38]. Our finding showed that PTS treatment significantly increased the intracellular GSH level compared with the  $\text{H}_2\text{O}_2$ -treated group. With regard to embryo quality, PTS supplementation to IVC medium improved blastocyst quality by reducing the number of apoptotic cells and increasing the total cell number of blastocysts. Our results were similar to those of another study that shows that PTS decreased the apoptotic cell number by protecting the testicular ischemia-reperfusion injury in rats [39].

PTS mediated the activation of the KEAP1–NFE2L2 pathway against  $\text{H}_2\text{O}_2$ -induced oxidative stress in mouse embryos, thereby exerting a cytoprotective effect. Western blot analysis revealed the NFE2L2 protein translocation from the cytoplasm to the nucleus and activation of antioxidant enzymes. This finding was supported with resveratrol-elicited translocation of NFE2L2 to the nucleus [40]. The upregulation of NFE2L2-dependent antioxidant enzymes, such as *HMOX1*, *CAT*, *GPX*, and *SOD*, was noted. Our results were in accordance with that of Bhakkiyalakshmi *et al.* [28], who demonstrated that PTS activation of NFE2L2 pathway conferred protection of antioxidant response (*SOD*, *CAT*, and *GPX*) and detoxification (*HMOX1*, *NQO1*, and *GCS*) against streptozotocin (STZ)-induced pancreatic beta cells. Recently, Sireesh *et al.* [25] reported that PTS improved beta-cell function and survival against cytokine stress and prevented STZ diabetes via NFE2L2 signaling cascade. We showed here that the improved expression of NFE2L2 downstream antioxidant genes, such as *HMOX1*, *CAT*, *GPX*, and *SOD*, subdued oxidative damage by scavenging free radicals, thereby protecting early preimplantation mouse embryos [4]. In this study, we also investigated apoptosis-related genes because  $\text{H}_2\text{O}_2$  causes programmed cell death [41]. PTS treatment with  $\text{H}_2\text{O}_2$  induced oxidative stress, showing significant increase in the expression of the anti-apoptotic gene *BCL2*. Meanwhile, PTS reduced the expressions of pro-apoptotic genes *BAX* and effector *Caspase-3*. Furthermore, Western blot analysis of BAX protein showed the downregulation by PTS and BCL-2 upregulation in mouse blastocyst confirmed the protective effect of PTS. A similar observation was reported in induced diabetic animals as PTS improved the *BCL2* and dampened the *Caspase-3* and *BAX* expression by NFE2L2 activation in pancreatic  $\beta$ -cells against various insults, such as cytokines and oxidative stress [25]. All these results indicated the significance of NFE2L2 downstream antioxidant response activated by PTS.

In conclusion, the present study demonstrated that 0.25  $\mu\text{M}$  supplementation of PTS in the IVC medium improved the development

competence and quality of mouse embryos, enhanced survival via the NFE2L2 signaling pathway, decreased the ROS levels, increased the GSH levels, and reduced the apoptotic index and rate in the mouse blastocyst. These results verified the potential role of PTS as an antioxidant during *in vitro* embryo development.

## Acknowledgments

The authors wish to thank the following people for their help: Zhang-Ze Qian and He-Li Na. This work was supported by The National Natural Science Foundation of China (Project No. 31360546).

## References

1. Quideau S, Deffieux D, Douat-Casassus C, Pouységú L. Plant polyphenols: chemical properties, biological activities, and synthesis. *Angew Chem Int Ed Engl* 2011; **50**: 586–621. [Medline] [CrossRef]
2. Hu JP, Calomme M, Lasure A, De Bruyne T, Pieters L, Vlietinck A, Vanden Berghe DA. Structure-activity relationship of flavonoids with superoxide scavenging activity. *Biol Trace Elem Res* 1995; **47**: 327–331. [Medline] [CrossRef]
3. Kerry NL, Abbey M. Red wine and fractionated phenolic compounds prepared from red wine inhibit low density lipoprotein oxidation *in vitro*. *Atherosclerosis* 1997; **135**: 93–102. [Medline] [CrossRef]
4. Lin C, Yon JM, Jung AY, Lee JG, Jung KY, Kang JK, Lee BJ, Yun YW, Nam SY. Resveratrol prevents nicotine-induced teratogenesis in cultured mouse embryos. *Reprod Toxicol* 2012; **34**: 340–346. [Medline] [CrossRef]
5. Ovesná Z, Kozics K, Bader Y, Saiko P, Handler N, Erker T, Szekeres T. Antioxidant activity of resveratrol, piceatannol and 3,3',4,4',5,5'-hexahydroxy-trans-stilbene in three leukemia cell lines. *Oncol Rep* 2006; **16**: 617–624. [Medline]
6. Lin HS, Yue BD, Ho PC. Determination of pterostilbene in rat plasma by a simple HPLC-UV method and its application in pre-clinical pharmacokinetic study. *Biomed Chromatogr* 2009; **23**: 1308–1315. [Medline] [CrossRef]
7. Rimando AM, Cuendet M, Desmarchelier C, Mehta RG, Pezzuto JM, Duke SO. Cancer chemopreventive and antioxidant activities of pterostilbene, a naturally occurring analogue of resveratrol. *J Agric Food Chem* 2002; **50**: 3453–3457. [Medline] [CrossRef]
8. Stivala LA, Savio M, Carafoli F, Perucca P, Bianchi L, Maga G, Forti L, Pagnoni UM, Albini A, Prosperi E, Vannini V. Specific structural determinants are responsible for the antioxidant activity and the cell cycle effects of resveratrol. *J Biol Chem* 2001; **276**: 22586–22594. [Medline] [CrossRef]
9. Remsburg CM, Yáñez JA, Ohgami Y, Vega-Villa KR, Rimando AM, Davies NM. Pharmacometrics of pterostilbene: preclinical pharmacokinetics and metabolism, anticancer, antiinflammatory, antioxidant and analgesic activity. *Phytother Res* 2008; **22**: 169–179. [Medline] [CrossRef]
10. Cichoński M, Paluszczak J, Szafer H, Piechowiak A, Rimando AM, Baer-Dubowska W. Pterostilbene is equally potent as resveratrol in inhibiting 12-O-tetradecanoylphorbol-13-acetate activated NF $\kappa$ B, AP-1, COX-2, and iNOS in mouse epidermis. *Mol Nutr Food Res* 2008; **52**(Suppl 1): S62–S70. [Medline]
11. Kapetanovic IM, Muzzio M, Huang X, Thompson TN, McCormick DL. Pharmacokinetics, oral bioavailability, and metabolic profile of resveratrol and its dimethylether analog, pterostilbene, in rats. *Cancer Chemother Pharmacol* 2011; **68**: 593–601. [Medline] [CrossRef]
12. Amarnath Sathesh M, Pari L. The antioxidant role of pterostilbene in streptozotocin-nicotinamide-induced type 2 diabetes mellitus in Wistar rats. *J Pharm Pharmacol* 2006; **58**: 1483–1490. [Medline] [CrossRef]
13. Nikhil K, Sharan S, Roy P. A pterostilbene derivative suppresses osteoclastogenesis by regulating RANKL-mediated NF $\kappa$ B and MAPK signaling in RAW264.7 cells. *Pharmacol Rep* 2015; **67**: 1264–1272. [Medline] [CrossRef]
14. Whitworth KM, Li R, Spate LD, Wax DM, Rieke A, Whyte JJ, Manandhar G, Sutovsky M. Method of oocyte activation affects cloning efficiency in pigs. *Mol Reprod Dev* 2009; **76**: 490–500. [Medline] [CrossRef]
15. Rizo D, Clemente M, Bermejo-Alvarez P, de La Fuente J, Lonergan P, Gutiérrez-Adán A. Consequences of *in vitro* culture conditions on embryo development and quality. *Reprod Domest Anim* 2008; **43**(Suppl 4): 44–50. [Medline] [CrossRef]
16. Duranthon V, Watson AJ, Lonergan P. Preimplantation embryo programming: transcription, epigenetics, and culture environment. *Reproduction* 2008; **135**: 141–150. [Medline] [CrossRef]



17. **de Matos DG, Furnus CC.** The importance of having high glutathione (GSH) level after bovine in vitro maturation on embryo development effect of  $\beta$ -mercaptoethanol, cysteine and cystine. *Theriogenology* 2000; **53**: 761–771. [Medline] [CrossRef]
18. **Mukherjee A, Kumar D, Singh KP, Chauhan MS, Singla SK, Palta P, Manik RS.** Assessment of DNA damage during in vitro development of buffalo (*Bubalus bubalis*) embryos: effect of cysteamine. *Reprod Domest Anim* 2010; **45**: 1118–1121. [Medline] [CrossRef]
19. **Wang F, Tian X, Zhang L, Tan D, Reiter RJ, Liu G.** Melatonin promotes the in vitro development of pronuclear embryos and increases the efficiency of blastocyst implantation in murine. *J Pineal Res* 2013; **55**: 267–274. [Medline] [CrossRef]
20. **Chen Z, Zuo X, Li H, Hong R, Ding B, Liu C, Gao D, Shang H, Cao Z, Huang W, Zhang X, Zhang Y.** Effects of melatonin on maturation, histone acetylation, autophagy of porcine oocytes and subsequent embryonic development. *Anim Sci J* 2017; **88**: 1298–1310. [Medline] [CrossRef]
21. **Wang F, Tian X, Zhang L, He C, Ji P, Li Y, Tan D, Liu G.** Beneficial effect of resveratrol on bovine oocyte maturation and subsequent embryonic development after in vitro fertilization. *Fertil Steril* 2014; **101**: 577–586. [Medline] [CrossRef]
22. **Spricigo JF, Morató R, Arcarons N, Yeste M, Dode MA, López-Bejar M, Mogas T.** Assessment of the effect of adding L-carnitine and/or resveratrol to maturation medium before vitrification on in vitro-matured calf oocytes. *Theriogenology* 2017; **89**: 47–57. [Medline] [CrossRef]
23. **Chiou YS, Tsai ML, Nagabhushanam K, Wang YJ, Wu CH, Ho CT, Pan MH.** Pterostilbene is more potent than resveratrol in preventing azoxymethane (AOM)-induced colon tumorigenesis via activation of the NF-E2-related factor 2 (Nrf2)-mediated antioxidant signaling pathway. *J Agric Food Chem* 2011; **59**: 2725–2733. [Medline] [CrossRef]
24. **Kosuru R, Kandula V, Rai U, Prakash S, Xia Z, Singh S.** Pterostilbene decreases cardiac oxidative stress and inflammation via activation of AMPK/Nrf2/HO-1 pathway in fructose-fed diabetic rats. *Cardiovasc Drugs Ther* 2018; **32**: 147–163. [Medline] [CrossRef]
25. **Sireesh D, Ganesh MR, Dhamodharan U, Sakthivadivel M, Sivasubramanian S, Gunasekaran P, Ramkumar KM.** Role of pterostilbene in attenuating immune mediated devastation of pancreatic beta cells via Nrf2 signaling cascade. *J Nutr Biochem* 2017; **44**: 11–21. [Medline] [CrossRef]
26. **He X, Chen MG, Ma Q.** Activation of Nrf2 in defense against cadmium-induced oxidative stress. *Chem Res Toxicol* 2008; **21**: 1375–1383. [Medline] [CrossRef]
27. **Yu S, Yan X, Liu H, Cai X, Cao S, Shen L, Zuo Z, Deng J, Ma X, Wang Y, Ren Z.** Improved establishment of embryonic stem (ES) cell lines from the Chinese Kunming mice by hybridization with 129 mice. *Int J Mol Sci* 2014; **15**: 3389–3402. [Medline] [CrossRef]
28. **Bhakkijalakshmi E, Shalini D, Sekar TV, Rajaguru P, Paulmurugan R, Ramkumar KM.** Therapeutic potential of pterostilbene against pancreatic beta-cell apoptosis mediated through Nrf2. *Br J Pharmacol* 2014; **171**: 1747–1757. [Medline] [CrossRef]
29. **Favetta LA, St John EJ, King WA, Betts DH.** High levels of p66shc and intracellular ROS in permanently arrested early embryos. *Free Radic Biol Med* 2007; **42**: 1201–1210. [Medline] [CrossRef]
30. **Gad A, Hoelker M, Besenfelder U, Havlicek V, Cinar U, Rings F, Held E, Dufort I, Sirard MA, Schellander K, Tesfaye D.** Molecular mechanisms and pathways involved in bovine embryonic genome activation and their regulation by alternative in vivo and in vitro culture conditions. *Biol Reprod* 2012; **87**: 100. [Medline] [CrossRef]
31. **Bhakkijalakshmi E, Sireesh D, Sakthivadivel M, Sivasubramanian S, Gunasekaran P, Ramkumar KM.** Anti-hyperlipidemic and anti-peroxidative role of pterostilbene via Nrf2 signaling in experimental diabetes. *Eur J Pharmacol* 2016; **777**: 9–16. [Medline] [CrossRef]
32. **Elango B, Dornadula S, Paulmurugan R, Ramkumar KM.** Pterostilbene ameliorates streptozotocin-induced diabetes through enhancing antioxidant signaling pathways mediated by Nrf2. *Chem Res Toxicol* 2016; **29**: 47–57. [Medline] [CrossRef]
33. **Chakraborty A, Gupta N, Ghosh K, Roy P.** In vitro evaluation of the cytotoxic, anti-proliferative and anti-oxidant properties of pterostilbene isolated from *Pterocarpus marsupium*. *Toxicol In Vitro* 2010; **24**: 1215–1228. [Medline] [CrossRef]
34. **Moon D, McCormack D, McDonald D, McFadden D.** Pterostilbene induces mitochondrially derived apoptosis in breast cancer cells in vitro. *J Surg Res* 2013; **180**: 208–215. [Medline] [CrossRef]
35. **Held E, Salilew-Wondim D, Linke M, Zechner U, Rings F, Tesfaye D, Schellander K, Hoelker M.** Transcriptome fingerprint of bovine 2-cell stage blastomeres is directly correlated with the individual developmental competence of the corresponding sister blastomere. *Biol Reprod* 2012; **87**: 154. [Medline] [CrossRef]
36. **Xue EX, Lin JP, Zhang Y, Sheng SR, Liu HX, Zhou YL, Xu H.** Pterostilbene inhibits inflammation and ROS production in chondrocytes by activating Nrf2 pathway. *Oncotarget* 2017; **8**: 41988–42000. [Medline]
37. **Hayes JD, Flanagan JU, Jowsey IR.** Glutathione transferases. *Annu Rev Pharmacol Toxicol* 2005; **45**: 51–88. [Medline] [CrossRef]
38. **Wang B, Liu H, Yue L, Li X, Zhao L, Yang X, Wang X, Yang Y, Qu Y.** Neuroprotective effects of pterostilbene against oxidative stress injury: Involvement of nuclear factor erythroid 2-related factor 2 pathway. *Brain Res* 2016; **1643**: 70–79. [Medline] [CrossRef]
39. **Kim HJ, Lee JW, Hwang BR, Lee YA, Kim JI, Cho YJ, Jhun HJ, Han JS.** Protective effect of pterostilbene on testicular ischemia/reperfusion injury in rats. *J Pediatr Surg* 2016; **51**: 1192–1196. [Medline] [CrossRef]
40. **Hsieh TC, Lu X, Wang Z, Wu JM.** Induction of quinone reductase NQO1 by resveratrol in human K562 cells involves the antioxidant response element ARE and is accompanied by nuclear translocation of transcription factor Nrf2. *Med Chem* 2006; **2**: 275–285. [Medline] [CrossRef]
41. **Yang HW, Hwang KJ, Kwon HC, Kim HS, Choi KW, Oh KS.** Detection of reactive oxygen species (ROS) and apoptosis in human fragmented embryos. *Hum Reprod* 1998; **13**: 998–1002. [Medline] [CrossRef]